A DFT Study on Isomorphously Substituted MCM-22 Zeolite

Yan Wang, Danhong Zhou, Gang Yang, Shaojun Miao, Xiancun Liu, and Xinhe Bao*

State Key Laboratory of Catalysis, Dalian Institute of Chemical Physics, Chinese Academy of Sciences, Dalian, 116023, Liaoning, China

Received: December 2, 2003; In Final Form: March 15, 2004

The density functional theory has been used to study the isomorphously substituted MCM-22 zeolite for the first time. The effect of the basis sets on the calculation results is discussed in details. Data of several index properties for characterizing the relative acidity of T−MCM-22 (T = B, Al, Ga, and Fe), including proton affinity, bond length and bond angle, OH stretching frequency, and charge on the acidic proton, show that the acidity of T−MCM-22 increases in the sequence of B−MCM-22 < Fe−MCM-22 < Ga−MCM-22 < Al−MCM-22. After making a correction, the calculated OH stretching frequencies for Al−MCM-22 and Fe−MCM-22 show a reasonable agreement with the experimental data. On the basis of an equilibrium structure of the B−MCM-22 zeolite, the effect of the B element in the synthesis of the Ti−MCM-22 is also discussed. The adding of the B element during the synthesis of the Ti−MCM-22 can decrease greatly the Ti substitution energy because of the forming of a structure quite similar to the terminal silanol group. The results can provide some constructively information for zeolite synthesis.

Introduction

MCM-22 is a relatively new member in the family of zeolite, which consists of two series of independent porous structures: a 10-MR (member ring) sinusoidal (4.0 × 5.9 Å diameters) and a 12-MR supercage (7.1 × 18.1 Å) interconnected through 10-MR windows.[1,2] The unique pore configuration of this zeolite indicates its promising application in catalysis.[3−6] However, the lack of catalytically active sites in this structure limits its realization, and only a few catalytic processes in laboratory scale have be reported up to now. For improving, the isomorphous substitution with other trivalent elements, such as B, Ga, and Fe, has been used to modify its acidity and pore structure. B−MCM22, also referred to as ERB-1, was first synthesized in 1988. It displays intercalation properties toward polar molecules.[7,8] The first description of Ga−MCM-22 synthesis was in 1995 by Morrison et al.,[9] and a good performance in catalytic dehydrogenation of methylcyclohexane to toluene was reported simultaneously. Another important example is Fe−MCM-22, which was reported by Wu et al.[10] in 1997 and revealed a better selectivity for oxidative dehydrogenation and for selective catalytic reduction (SCR) of NO with NH_3 in the presence of O_2. However, the difficulties derived mainly from the minor amount of the modifying elements in the framework of the MCM-22 suppress the experimental investigation on their properties, such as activity and structural variations. Wu et al. investigated the Brønsted acidity of the Fe−MCM-22 zeolite by using infrared (IR) spectroscopy and pyridine adsorption and showed only the qualitative result, which was much weaker than that of Al−MCM-22 zeolite.[10] By studying the acidity of Fe- and [Fe, Al]−MCM-22 zeolites, Testa et al.[11] received a similar result, and no structure data referring to T−MCM-22 (T = B, Fe, Ga) has been announced so far.

Recently, many studies have shown that quantum mechanical calculations can yield useful information for predicting the acidity and structures of the isomorphously substituted zeolites.[12−18] However, no calculation is reported for isomorphously substituted MCM-22 zeolites so far. Moreover, among the calculations which have studied the isomorphously substituted zeolites by quantum mechanical methods, there is almost no calculation on the OH stretching frequencies except one article with a less reliable method or model,[16] since the frequency calculations need enormous computational resources. In this work, the Brønsted acidity of isomorphously substituted MCM-22 zeolites is studied by the density functional theory (DFT) for the first time. Besides the PA data, geometric parameters, and charge analysis, the OH stretching frequencies are also calculated with the reliable model and methods to directly relate it with the experimental IR spectroscopy, which, to our knowledge, is lacking. On the basis of an equilibrium structure of the B−MCM-22 zeolite, the effect of B element in the synthesis of the Ti−MCM22 zeolite is also investigated.

Models and Methods

In this work, the model which we chose included eight T (Si, T) atoms and was centered with the O atom in the form of $(H_3SiO)_3Si-(H)O-T(OSiH_3)_3$. The cluster geometry was assumed according to the crystal structure of hexagonal MWW type MCM-22 zeolite. We believed that our cluster model was enough for calculation since the previous work[19−21] and our recent paper[22] have gotten the reliable results with the size of the model. In the optimization, the outermost two coordination shells were held fixed in their crystallographic position,[23] and the rest of the atoms were fully optimized. The crystallographic labeling of pure silica MCM-22 is in accordance with "Atlas of Zeolite Framework Types" proposed by Koningsveld et al.,[23] but is different from the labeling by Sastre et al.[25] Recently, both our group [22,24] and Sastre et al.[25] have proved that the T4 sites is one of the most preferred locations for aluminum substitution in the MCM-22 zeolite, so in this work, we have focused on T4 site to perform the calculations.

The relative acidity of isomorphously substituted MCM-22 zeolites in this work was performed by the nonlocal gradient-corrected B3LYP density functional theory (DFT) with the Gaussian 98 program. Zygmunt et al.[26] have shown that this

* Corresponding author. Tel: 086-0411-4686637; fax: 086-0411-4694447; e-mail: xhbao@dicp.ac.cn.

10.1021/jp0376875 CCC: $27.50
Published on Web 07/20/2004

TABLE 1: The Calculated Total Energies (*E*, hartree) and Proton Affinity (PA, kcal/mol) for the T−MCM-22 Zeolite

method		Al	Ga	Fe	B
(U)B3LYP/6-31g*	EZOH	−2804.1618	−4484.5674	−3825.1929	−2586.5304
	EZO-	−2803.6468	−4484.0497	−3825.6754	−2585.9831
	PA	323.1	324.8	324.7	343.4
(U)B3LYP/6-311g*	EZOH	−2804.5987	−4486.8916	−3825.6869	−2586.9506
	EZO-	−2804.0878	−4486.3702	−3825.1724	−2586.4082
	PA	320.6	321.5	322.8	340.4
(U)B3LYP/6-311+g**	EZOH	−2804.6587	−4486.95013	−3825.7661	−2587.0125
	EZO-	−2804.1485	−4486.4388	−3825.2528	−2586.4722
	PA	320.2	320.9	322.1	339.1

method constitutes the best choice for DFT treatment of zeolite systems. To test the effect of the basis set, three basis sets, including 6-31g*, 6-311g*, and 6-311+g**, were adopted. All of the models were optimized using spin-restricted procedures, except for the models containing Fe which are open-shell systems and were calculated with a spin multiplicity of six. It was confirmed from computed $<S^2>$ values that spin contamination included in the calculation is neglectable after annihilation of higher spin states. The frequency and charge analysis were carried out on the basis of the optimization results. The detailed models and methods for considering the effect of the B element in the synthesis of the Ti−MCM-22 zeolite are presented in part 5 of the Results and Discussion section below.

Results and Discussion

1. The Proton Affinity (PA) of the T−MCM-22 Zeolites. It is well known that the proton affinity is a good measure of the relative acidity for the models of substituted zeolites. Models with high proton affinity are poor proton donors and hence have a low Brønsted acidity. On the contrary, models with a low proton affinity are better proton donors and are more acidic. The proton affinity of isomorphously substituted MCM-22 zeolites can be reasonably approximated by the reaction ZOH $\rightarrow ZO^- + H^+$, where ZO^- and ZOH represent the deprotonated and the neutral zeolites, respectively. To investigate the dependence of the proton affinity (PA) on the basis sets, calculations with B3LYP/6-31g*, B3LYP/6-311g*, and B3LYP/6-311+G** were carried out.

Table 1 summarizes the calculated total energies and PA data of T−MCM-22 zeolites with the different basis sets, where T atoms represent Al, Ga, Fe, and B, respectively. It was observed that as the 6-31g* basis set was applied, the PA value of the boron-substituent cluster was much higher than those for other T−MCM-22 zeolites and the PA value of Ga−MCM-22 zeolite was slightly higher than that of Fe−MCM-22 zeolite. The Al−MCM-22 zeolite gave the minimum PA value. When the basis set was increased to the 6-311g*, the PA value of the boron-substituent cluster exhibited the same behavior as that by the 6-31g* basis set, namely, still much higher than those for other T−MCM-22 zeolites. However, the calculated PA value of Ga−MCM-22 became smaller than that of the Fe−MCM-22 zeolite and the calculated PA data for T−MCM-22 zeolites showed the sequence Al−MCM-22 < Ga−MCM-22 < Fe−MCM-22 < B−MCM-22. Moreover, the PA data decreased by 2.56, 3.33, 1.94, and 3.04 kcal/mol for the Al−MCM-22, Ga−MCM-22, Fe−MCM-22, and B−MCM-22, respectively, as compared with the 6-31g* basis set. After further increase of the basis set to the 6-311+g** by adding additional polarization and diffuse function to the hydrogen, the calculated PA data of T−MCM-22 zeolites showed the same sequence as that given by the 6-311g* basis sets and gave even smaller changes, as compared with the values given by the 6-311g* basis sets. The PA difference calculated by the 6-311g* and 6-311+g** basis set decreased to 0.39, 0.66, 0.66, and 1.29 kcal/mol for Al, Ga, Fe, and B−MCM-22, respectively. Thus, the PA data appeared to converge with the expanding of the basis sets. So, we conclude that the 6-311g* as well as the further enlarged 6-311+g** basis set can give more accurate results, as compared to the 6-31g* basis set, and the trend of the relative acid strength of the T−MCM-22 zeolites can be predicted as Al−MCM-22 > Ga−MCM-22 > Fe−MCM-22 > B−MCM-22, which was consistent with the calculation result of T-ZSM-5 zeolites obtained by the theoretical calculations[12−18] and experiments.[27] The sequence of relative acid strength of the T−MCM-22 zeolite is also consistent with the Pauling electronegativities of trivalent substitution elements which have the same order: $X_{Al}{}^a$ (1.61) < $X_{Ga}{}^a$ (1.81) < $X_{Fe}{}^a$ (1.83) < $X_B{}^a$ (2.04).[28] Because the electronegativity of B element is much higher than that of other elements, it also makes clear the reason that the PA values of the boron substituent were much higher than those of other T−MCM-22 zeolites.

TABLE 2: The Selected Geometric Parameters of the T−MCM-22 Zeolite with (U)B3LYP/6-31g*

bond and angle	Al	Ga	Fe	B
*d*O−H	0.972	0.972	0.972	0.966
*d*T−O	1.840	1.920	1.940	2.110
*d*Si−O	1.670	1.670	1.670	1.630
∠T−O−Si	126.7	121.4	118.4	131.0

TABLE 3: The Selected Geometric Parameters of the T−MCM-22 Zeolite with (U)B3LYP/6-311g*

bond and angle	Al	Ga	Fe	B
*d*O−H	0.964	0.963	0.962	0.960
*d*T−O	1.830	1.910	1.930	2.000
*d*Si−O	1.660	1.660	1.650	1.620
∠T−O−Si	127.0	123.1	119.0	135.9

2. The Geometric Parameters of the T−MCM-22 Zeolites. In this section, we try to find a close relation between the geometric parameters and the acidity of T−MCM-22 zeolites. Table 2 lists the key bond lengths and angles for the equilibrium geometries of T−MCM-22 zeolites by 6-31g* basis set. It can be seen that the distances between the bridging oxygen and the protonic H atoms (d_{O-H}) are almost unchanged (0.972 Å) for Al, Ga, and Fe substitution. However, when the silicon was substituted by a boric atom, the O−H bond lengths decreased from 0.972 Å to 0.966 Å. The distances between the bridging oxygen and the silicon atoms (d_{Si-O}) exhibited a behavior very similar to that of the O−H bonds. The Si−O bond lengths are all lengthened to 1.670 Å compared to the Si−O bond distance in the siliceous models, as the Si was substituted by Al, Ga, and Fe. When a boric atom was introduced into the zeolite framework, the Si−O bond length decreased to 1.630 Å. Unlike the d_{O-H} and d_{Si-O}, the substituent atoms appeared to cause significant changes in the distances between the bridging oxygen and T atoms (d_{O-T}) for all T−MCM-22 zeolites and the distances between the bridging oxygen and T atoms (d_{O-T}) increased with the order Al−MCM-22 < Ga−MCM-22 < Fe−MCM-22 < B−MCM-22, consistent with the calculated PA data of the T−MCM-22 zeolites obtained with the 6-311g* and the 6-311+g** basis set. To consider the effect of basis set on the equilibrium structures, the results by two other basis sets, namely, 6-311g* and 6-311+g**, are presented in Tables 3 and 4. Unlike the results obtained by 6-31g* basis set (d_{O-H} is almost unchanged for Al, Ga, and Fe substitution), the d_{O-H} of MCM-22 zeolites with different heteroatoms can be well distinguished and is well related to the type of trivalent substitution atoms. Namely, the d_{O-H} decreased slightly in the same trend of the

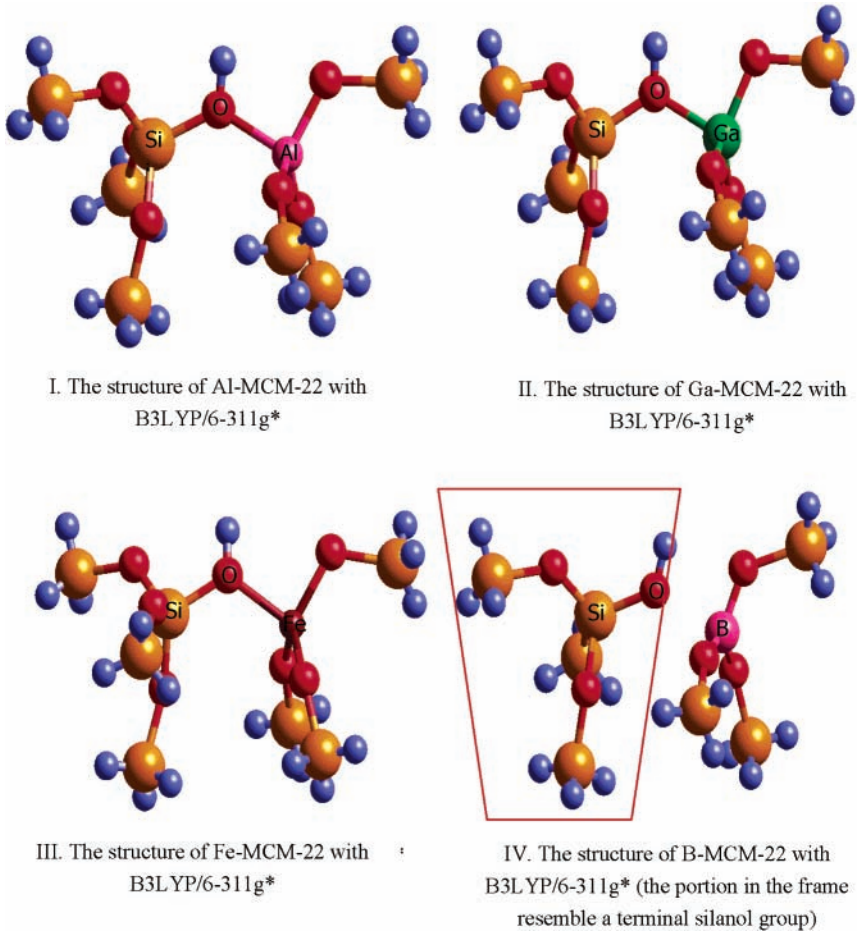

Figure 1. The structures of T−MCM-22 by B3LYP/6-311g* method.

TABLE 4: The Selected Geometric Parameters of the T−MCM-22 Zeolite with (U)B3LYP/6-311+g**

bond and angle	Al	Ga	Fe	B
*d*O−H	0.966	0.965	0.965	0.961
*d*T−O	1.820	1.910	1.940	2.020
*d*Si−O	1.660	1.660	1.660	1.630
∠T−O−Si	127.0	122.9	117.7	134.6

TABLE 5: The Calculated OH Stretching Frequency (cm^{-1}) for the T−MCM-22 Zeolite

method	Al	Ga	Fe	B
(u)B3LYP/6-31g*	3762.2	3764.5	3767.8	3827.5
(u)B3LYP/6-311g*	3825.4	3833.0	3851.7	3875.8
(u)B3LYP/6-311$^+$g**	3828.2	3833.4	3834.6	3888.6
IR expriment	3621		3637	

order of acid strength of T−MCM-22 zeolites (Al > Ga > = Fe > B). From the above data, we considered that the 6-311g* or larger basis sets should be applied to correctly and clearly distinguish the differences in the structures and the acidity of T−MCM-22 zeolites.

For T = B, however, we can see from Tables 2−4 that the angles of B−O−Si are not consistent with the sequence of the PA data or the acid strength of T−MCM-22 zeolites, and the angle of B−O−Si increases even more than that of Al−MCM-22 zeolite. This might be ascribed to the small size of B^{3+} cation. From the calculation, we found that the sum of the OBO angle of the three short B−O bonds in the B−MCM-22 zeolite is much closer to 360° than that of Al, Ga, and Fe−MCM-22 and B is far removed from the bridging hydroxyl group (the calculated B−O bond lengths are from 2.000 to 2.110 Å for different basis sets), seeing Figure 1.IV. Thus, it indicated that there is almost no bonding between the B and the bridging oxygen and a structure closely resembling a terminal silanol group is formed in the [B]−MCM-22 zeolite, which led to the abnormality of the angles of B−O−Si. Those results agree well with the DFT calculations on B−ZSM-5 and B-Mazzite by Chatterjee,[15] Stave,[18] and Valerio.[19] They considered that when a proton is associated with a boron element, the tetrahedral BO4 unit is replaced by a trigonal BO_3 entity and a silanol group is formed on the adjacent silicon.

3. The OH Stretching Frequencies of the T−MCM-22 Zeolites (γ_{OH}). It has been generally accepted that the stretching vibrational frequencies for the O−H bonds can also reflect the acidity of the T−MCM-22 zeolites. Lower wavenumbers of r_{OH} are related to weaker O−H bond strengths and hence correspond to stronger acid strength. However, because it requires enormous computational resources, the DFT calculation on the OH stretching frequencies of the zeolites is very limited. In this work, the calculated stretching vibrational frequencies for the O−H bond by three different basis sets are given in Table 5. Unlike the proton affinity and the structure parameters of the equilibrium geometries, the calculated stretching vibrational frequencies obtained by the 6-31g* basis set are in agreement with the sequence of the acid strength of T−MCM-22 zeolites, namely, for the r_{OH}: Al−MCM-22 < Ga−MCM-22 < Fe−MCM-22 < B−MCM-22, and for the acidity: Al−MCM-22 > Ga−MCM-22 > Fe−MCM-22 > B−MCM-22. Increasing the basis set to 6-311g* and 6-311+g** gave no change in the relative order of the acid strength of the T−MCM-22 zeolites. Moreover, with different basis sets, the calculated vibrational frequencies for B−MCM-22 zeolite were always much higher

TABLE 6: The Mulliken and NBO Population Analysis of the T−MCM-22 Zeolite

(u)B3LYP/ 6-311g*	atom	Al	Ga	Fe	B
Mulliken	q_T	1.147283	1.340077	1.736223	0.633464
	q_O	−0.890782	−0.924701	−0.914049	−0.816044
	q_H	0.518712	0.516033	0.493273	0.455321
NBO	q_T	1.99464	1.82190	1.90211	1.36589
	q_O	−1.10289	−1.07724	−1.10363	−1.05423
	q_H	0.55303	0.54848	0.53931	0.52817

than those of the other T−MCM-22 zeolites, just like the calculated PA data. These results may indicate that 6-31g* basis set is quite enough for frequency calculation. The results are similar to the previous quantum mechanics calculations, in which the author considered that the OH stretching frequencies were much less dependent on model size than on the proton affinity.[29]

The gaps between the calculated vibrational frequencies for different T−MCM-22 zeolites correlate well with the structure parameters. For example, the r_{OH} differences between the Ga−MCM-22 and Fe−MCM-22 zeolite calculated by 6-31g* and 6-311+g** basis sets are much slighter than that by 6-311g* basis set, seeing Table 5. Correspondingly, the O−H bond length of Ga−MCM-22 zeolite is much larger than that of the Fe−MCM-22 obtained by the 6-311g* basis set, while by the 6-31g* and 6-311+g** basis sets, the differences of the O−H bond lengths between Ga−MCM-22 and Fe−MCM-22 are very small, as shown in Tables 2−4.

It is well known that the vibrational frequencies calculated by 6-31g* basis set should be scaled by a factor of 0.9614.[30] After making a correction, we found that the vibrational frequencies of 3617 cm^{-1} and 3622 cm^{-1} are reasonably in agreement with the experimental results of 3621 cm^{-1} for Al−MCM-22 zeolite and 3637 cm^{-1} for Fe−MCM-22 zeolite. It is regrettable that no experimental O−H stretching frequencies for B−MCM-22 and Ga−MCM-22 zeolite have yet been reported. These results further identify that the T4 site which we have chosen for the calculation is reasonable. To be consistent with the scaled B3LYP/6-31g* frequencies, we assessed the 6-311g* and 6-311+g** should by scaled by 0.9455 and 0.9448, respectively.

4. The Charge Analysis of the T−MCM-22 Zeolites. The other index for characterizing the relative acidity of T−MCM-22 zeolites is the partial charges on the T−MCM-22 zeolites. In this part, only the 6-311g* basis set is applied since this basis set is enough for this system on the basis of the above calculation results. Table 6 listed the Mulliken and NBO population analysis for trivalent substitution atoms, bridge oxygens, and protonic H atoms. Although NBO analysis uses the natural orbital rather than the molecular orbital directly and can be less basis set dependent than the Mulliken scheme, we obtained similar results by Mulliken and NBO population analysis. It is well known that the increase of the charge on the proton (q_H) corresponds to the increase of the ionicity, and thus, to the increase of the acidity, so it can be stated from the q_H data listed in Table 6 that the acid strength of the substituted MCM-22 zeolites increases in the order of B−ZSM-5 < Fe−MCM-22 < Ga−ZSM-5 < Al−ZSM-5, which shows a high consistency with the calculated PA, the geometric parameters, and O−H stretching frequencies. We also found that there is no reflection of the acidity trend on the charges of any atoms other than the acidic proton by both Mulliken and NBO population analysis.

5. The Effect of B Element in the Synthesis of the Ti−MCM-22 Zeolite. The zeolites in which the framework Si atoms are substituted by Ti atoms are heterogeneous environmentally friendly catalysts. The microporous titanosilicate (TS-1), discovered in the early 1980s,[31] has become one of the most relevant heterogeneous industrial catalysts in the last twenty years because of its remarkable high efficiency and molecular selectivity in oxidation reactions.[32−34] However, the medium-size pores of TS-1 restrict their use to substrates and oxidants both with relatively small molecular diameters.[35−37] A novel titanosilicate with the MWW topology, first synthesized in 2000 by Wu et al., has overcome the disadvantage.[38−39] Different from the other zeolites containing Ti in the framework, the synthesis of the titanosilicate with the MWW topology must be conducted in the presence of boron element, so it is necessary to understand the effect of the boron element during the synthesis of the titanosilicate zeolite with the MWW topology.

TABLE 7: The Calculated Energies and Substitution Energies by Model A and Model B

	E_{Si} (hartree)[a]	E_{Ti} (hartree)[b]	E_{sub}(hartree)	ΔE_{sub}(kcal/mol)
model A	−1463.7650	−2023.7324	0.3958	17.6
model B	−1753.9828	−2313.9220	0.4239	

[a] $E_{si}^{4+} = -285.5779$ (hartree). [b] $E_{Ti}^{4+} = -845.9410$ (hartree).

As calculated above, the B atoms prefer tri- rather than tetra-coordination in the MCM-22 zeolite, and a structure which closely resembles a terminal silanol group is formed on the adjacent silicon when the B atoms are incorporated into the framework of the MCM-22 zeolite. Thus, to reduce the calculation time, a cluster model A, $(H_3SiO)_3$-T-OH, with a terminal silanol group was applied to approximately represent the structure synthesized in the presence of boron. For the synthesis in the absence of boron element, a cluster model B, $(H_3SiO)_4$-T, was chosen. The calculation was also performed by the nonlocal gradient-corrected B3LYP density functional theory (DFT) with the Gaussian 98 program. To reduce the calculation time, only the 6-311g* basis set was applied. The optimization process was the same as that of the calculation for the relative acidity of T−MCM-22 zeolite. The calculated substitution energies for the replacement of a silicon atom by a Ti atom in MCM-22 zeolite are shown in Table 7, which were determined by comparing the energies of the relaxed Si clusters to that of the corresponding relaxed Ti clusters. For the situation synthesized in the presence of boron, the substitution energy E_{sub} corresponds to the energy change of the reaction $(H_3SiO)_3-Si-OH + Ti^{4+} \rightarrow (H_3SiO)_3-Ti-OH + Si^{4+}$. The substitution energy E_{sub} representing the sample synthesized in the absence of boron was defined as the energy change of the reaction $(H_3SiO)_4-Si + Ti^{4+} \rightarrow (H_3SiO)_4-Ti + Si^{4+}$. The ΔE_{sub} data correspond to the difference of the substitution energies between the synthesis in the presence of boron and that in the absence of boron. The difference is quite large, about 17 kcal/mol, which suggests that the replacement of the Si by Ti in the presence of boron in the MCM-22 zeolite is much favored energetically than that in the absence of boron. From the above results, we can conclude that the adding of the B element can decrease greatly Ti substitution energy because of the forming of a structure closely resembling a terminal silanol group. From this point of view, the results also provide an understanding of the location of Ti atoms in MCM-22 framework: the preferential sitting of Ti atoms in the Ti−MCM-22 is to be adjacent to B atoms since the replacement of Si by Ti is much favored energetically in a structure closely resembling a terminal silanol group. While the cluster models investigated here for the synthesis of Ti−MCM-22 zeolite are approximate and relatively small, and the investigation with larger models or periodic ab initio techniques would arrive at more precise results, it can be assured that the

conclusions made in this paper will remain unchanged and provide some insight into the mechanism for the synthesis of Ti−MCM-22.

Conclusion

The density functional theory was used to study the structures and the Brønsted acidity of isomorphously substituted MCM-22 for the first time. The effect of the basis sets on the calculation results is discussed in details. By analyzing the proton affinity, the structures of optimized T−MCM-22 zeolite, the hydroxyl group vibrational frequencies, and the charge on acidic proton, we concluded that the acidity of T−MCM-22 zeolites increases according to the sequence B−MCM-22 < Fe−MCM-22 < Ga−MCM-22 < Al−MCM-22, which is consistent with the results of T−ZSM-5 zeolites by theoretical calculation and experiment. The calculated OH stretching frequencies are much less dependent on basis set than on the proton affinity and structures of T−MCM-22 zeolite. The OH stretching frequencies, 3617 cm^{-1} and 3622 cm^{-1} for Al−MCM-22 and Fe−MCM-22, respectively, show a reasonable agreement with the experimental data of 3621 cm^{-1} and 3637 cm^{-1}. On the basis of the equilibrium structure of the B−MCM-22 zeolite, the effect of B element in the synthesis of the Ti−MCM-22 zeolite was also studied. The difference of the substitution energies between the synthesis in the presence of boron and in the absence of boron is quite large, about 17 kcal/mol. Thus, the calculation clarified the reason for the adding of the B element in the synthesis of the Ti−MCM-22 zeolite, namely, the adding of the B element can decrease the Ti substitution energy greatly and is highly favorable energetically because of the forming of a structure which is closely similar to a terminal silanol group. We also predict that the Ti atoms in the Ti−MCM-22 locate preferentially in the neighborhood of the substituent B atoms. The results can provide some constructive information for zeolite synthesis.

Acknowledgment. This work was supported by the National Natural Science Foundation of China (Key Program: No 90206036) and the Ministry of Science and Technology of China (National Key Project of Fundamental Research: G1999022406). We acknowledge a grant of computer time at center for computational chemistry, State Key Lab of Molecular Reaction Dynamics, Dalian Institute of Chemical Physics.

References and Notes

(1) Rubin, M.; Chu, P. U.S. Patent. 4,954,325, 1990.
(2) Leononwica, M. E.; Lawton, J. A.; Rubin, M. K. *Science* **1994**, *264*, 1910.
(3) Aseni, A.; Corma, A.; Martinez, A. *J. Catal.* **199**6, *158*, 561.
(4) Ravishankar, R.; Sivasanker, S. *Appl. Catal. A* **1996**, *142*, 47.
(5) Corma, A.; Gonzàlez-Alfro, V.; Orchillès, A. V. *Appl. Catal. A* **1995**, *129*, 203.
(6) Corma, A.; Martinez-Triguero, J. *J. Catal.* **1997**, *165*, 102.
(7) Bellussi, G.; Perego, G.; Clerici, M. G.; Giusti, A. *Eurpat. Appl.* **1988**, 293032.
(8) Millini, R.; Perego, G.; Parker, W. O.; Bellussi, Jr.; Bellussi, G.; Carluccio, L. *Microporous Mater.* **1995**, *4*, 221.
(9) Morrison, R. A.; Rubin, M. K. U.S. Patent 5,382,742.
(10) Wu, P.; Komatsu, T.; Yashima, T. *Chem. Commun.* **1997**, 663.
(11) Testa, F.; Crea, F.; Diodati, G. D.; Pasqua, L.; Aiello, R.; Terwagne, G.; Lentz, P.; Nagy, J. B. *Microporous Mesoporous Mater.* **1999**, *30*, 187.
(12) O'Malley, P. J.; Dwyer, J. *Chem. Phys. Lett.* **1988**, *143*, 97.
(13) Viruela-Martin, P. M.; Zicovich-Wilson, C. M.; Corma, A. *J. Phys. Chem.* **1993**, *97*, 13713.
(14) Strodel, P.; Neyman, K. M.; Knözinger, H.; Rösch, N. *Chem. Phys. Lett.* **1995**, *240*, 547.
(15) Chatterjee, A.; Iwasaki, T.; Ebina, T.; Miyamoto, A. *Microporous Mesoporous Mater.* **1998**, *21*, 421.
(16) Yuan, S. P.; Wang, J. G.; Li, Y. W.; Peng, S. Y. *J. Mol. Catal. A-Chem.* **2002**, *178*, 267.
(17) Yuan, S. P.; Wang, J. G.; Li, Y. W.; Jiao, H. J. *J Phys. Chem. A* **2002**, *106*, 8167.
(18) Stave, M. S.; Nicholas, J. B. *J. Phys. Chem. B* **1995**, *99*, 15046.
(19) Valerio, G.; Goursot, A. *J. Phys. Chem. B* **1999**, *103*, 51.
(20) Valerio, G.; Plévert, J.; Goursot, A.; Renzo, F. D. *Phys. Chem. Chem. Phys.* **2000**, *2*, 1091.
(21) Ehresmann, J. O.; Wang, W.; Herreros, B.; Luigi, D.-P.; Venkatraman, T. N.; Song, W. G.; Nicholas, J. B.; Haw, J. F. *J. Am. Chem. Soc.* **2002**, *124*, 10868.
(22) Wang, Y.; Zhuang, J. Q.; Yang, G.; Zhou, D. H.; Han, X. W.; Bao, X. H. *J. Phys. Chem. B* **2004**, *108*, 1386.
(23) Meier, W. M.; Olson, D. H.; Baerlocher, C. *Altas of Zeolite Structure Type*, 4th ed.; Elsevier: Amsterdam, 1996; also on http://www.iza-structure.org/ databases/. The composition of the framework of MCM-22 zeolite given in the *Atlas of Zeolite Structure Type* is $[H^{+}_{2.4}\,Na^{+}_{3.1}]\,[Al_{0.4}B_{5.1}Si_{66.5}O_{144}]$.
(24) Zhou, D. H.; Wang, Y.; Ma, D.; Bao, X. H. *Chemical Journal of Chinese Universities*, the 8th quantum chemistry meeting, 2002; 207−211.
(25) Sastre, G.; Fornes, V.; Corma, A. *J. Phys. Chem. B* **2000**, *104*, 4349.
(26) Zygmunt, S. A.; Muller, R. M.; Curtiss, L. A.; Iton, L. E. *J. Mol. Strut.* **1998**, *430*, 9.
(27) Chu, Cynthia T-W.; Chang, C. D. *J. Phys. Chem.* **1985**, *89*, 1569;
(28) on http://www.webelements.com.
(29) Brand, H. V.; Curtiss, L. A.; Iton, I. E. *J. Phys. Chem.* **1992**, *96*, 7725.
(30) Scott, A. P.; Radom, L. *J. Phys. Chem.* **1996**, *100*, 16502.
(31) Taramasso, M.; Perego, G.; Notari, B. U.S. Patent 4410501, 1983.
(32) Ingallina, P.; Clerici, M. G.; Rossi, L.; Bellussi, G. *Stud. Surf. Sci. Catal.* **1994**, *92*, 31.
(33) Clerici, M. G.; Ingallina, P. *Catal. Today* **1998**, *41*, 251.
(34) Perego, C.; Carati, A.; Ingallina, P.; Mantegazza, M.; Bellussi, A. G. *Appl. Catal. A* **2001**, *221*, 63.
(35) Bellussi, G.; Carati, A.; Clerici, M. G.; Esposito, A.; Millini, R.; Buonomo, F. *BE* **1989**, 1001038.
(36) Reddy, J. S.; Kumar, R.; Ratnasamy, P. *Appl. Catal.* **1990**, *58*, L1.
(37) Serrano, D. P.; Hong-Xin, L. *J. Chem. Soc., Chem. Commun.* **1992**, 745.
(38) Wu, P.; Tatsumi, T.; Komatsu, T.; Yashima, T. *Chem. Lett.* **2000**, *7*, 774.
(39) Wu, P.; Tatsumi, T.; Komatsu, T.; Yashima, T. *J. Phys. Chem. B* **2001**, *105*, 2897.